Neural Correlates of Impaired Cognitive-Control over Working Memory in Schizophrenia

Supplemental Information

Supplemental Methods

Participants

Healthy controls (HCs), matched to patients for sex, age, education, and race, were recruited through local and online advertisements. They were free of current or past psychiatric or neurological illness, did not report alcohol or substance dependency in the last six months, and had not used psychotropic medication, such as antipsychotics or antidepressants, in the last year. Patients were recruited through the Lieber Center for Schizophrenia Research and Treatment of the New York State Psychiatric Institute (NYSPI) and all patients met DSM-IV criteria for schizophrenia (SZ) (S1). Diagnoses were determined through a diagnostic conference that included information from either the Diagnostic Instrument for Genetic Studies (S2) or the Structured Clinical Interview DSM-IV (S3). Additionally, the Scale for the Assessment of Positive Symptoms and the Scale for the Assessment of Negative Symptoms (S4), and the Calgary Depression Scale (S5) were used to evaluate symptom severity. Ratings were obtained between 2 weeks and 2 months from the testing day for 10 patients and more than 2 months but less than 5 months for 8 patients. All patients were being treated with atypical antipsychotic medication for at least three months, and had taken the same type and dose of medication for at least one month before the day of testing. All participants were English-speaking. All but two participants (one SZ, one HC) were right handed.

After the procedure was fully explained, written informed consent was obtained. Capacity to participate in the experiment was also assessed for each patient via an interview

process with a psychiatrist not related to the study. The research protocol was approved by the Institutional Review Board of the NYSPI and Columbia University.

Procedure

Experimental tasks were presented using E-Prime software (Psychology Software Tools, Inc., Pittsburgh, PA) and the Current Designs HH2x4-C system, with its 4-button response unit. Stimuli were projected onto a mirror above participant's eyes that was attached to the head coil.

fMRI Data Acquisition

Whole-brain imaging was conducted using a SENSE head coil on a 3.0T Phillips MRI system located at Columbia University's MRI Research Center. Head padding was used to minimize head motion; subsequent inspection showed that no participant's motion exceeded 2 mm in any direction from one volume acquisition to the next. Structural images were collected using a high-resolution T1-weighted MPRAGE pulse sequence (1 X 1 X 1 mm voxel size). Functional images were collected using a gradient echo T2*-weighted echoplanar sequence with blood oxygenation level-dependent contrast (TR = 2000 ms, TE = 20 ms, flip angle = 77, 3 X 3 X 2 mm voxel size; 52 contiguous axial slices). For each functional scanning run, five discarded volumes were collected prior to the first trial to allow for magnetic field equilibration.

Imaging Preprocessing and Analysis

Functional data were spike-corrected to reduce the impact of artifacts using AFNI's 3dDespike (http://afni.nimh.nih.gov/afni). Subsequent processing and analyses were done using SPM5 (http://www.fil.ion.ucl.ac.uk/spm/). Functional images were corrected for differences in

slice timing using sinc-interpolation, and head movement was corrected using a least-squares approach and a 6 parameter rigid body spatial transformation. Structural data were coregistered to the functional data and segmented into gray and white-matter probability maps (S6). These segmented images were used to calculate spatial normalization parameters to the Montreal Neurological Institute (MNI) template, which were subsequently applied to the functional data. As part of spatial normalization, the data were resampled to 2 x 2 x 2 mm^3. An 8-mm full-width/half-maximum isotropic Gaussian smoothing kernel was applied to all functional images prior to analysis using SPM5. All analyses included a temporal high-pass filter (128 s), correction for temporal autocorrelation using an autoregressive AR(1) model, and each image was scaled to have a global mean intensity of 100.

Ventrolateral Prefrontal Cortex Regions-of-Interest

Given our prior hypothesis, we focused the bulk of our analysis on the left ventrolateral prefrontal cortex (VLPFC). To do so, we first defined each region anatomically and then extracted data from voxels showing significant activation in the whole-brain analyses described in the main text. The left posterior VLPFC was defined as the left inferior frontal gyrus, pars opercularis and the left mid-VLPFC was defined as the left inferior frontal gyrus, pars triangularis according to demarcations provided by the Anatomical Automatic Labeling atlas implemented by WFU PickAtlas (S7). Group differences in the VLPFC were examined in two ways: first, we examined group differences averaging across all voxels demonstrating a significant effect in whole-brain analyses that collapsed across group. Second, heterogeneity within the VLPFC was explored by separately examining spherical regions of interest (ROIs) centered around each peak in the VLPFC reported in the whole-brain analyses that collapsed

across group. In this latter analysis, five peaks within left posterior VLPFC and three peaks within left mid-VLPFC were explored with the restriction that each peak was separated from all other peaks by at least 7 mm. Each spherical ROI had a 5 mm radius. These criteria resulted in each ROI being separated by other ROIs by at least a single voxel. Follow-up analyses exploring brain-brain and brain-behavioral relationships were estimated in the left posterior-VLPFC and mid-VLPFC spheres demonstrating maximal group differences. The left posterior VLPFC ROI was centered around (-50, 8, 22) and the left mid-VLPFC ROI was centered around (-40, 32, 22).

Supplemental Results

Examining Potential Motion Confounds

Recent data have indicated that differences in between-group motion can at times lead to spurious results (S8-S10). While these matters have been most directly addressed during resting state paradigms, motion may nevertheless confound task-based settings as well. Because no subject demonstrated more than a voxel of total displacement or 0.5 mm/degrees of inter-scan motion, we did not regress out motion explicitly in the analyses described in the main text. To more fully explore whether motion could have confounded our results, we calculated mean motion, maximum motion, mean rotation, and number of movements through methods described in van Djik *et al*., 2012 (S8). Patients and HCs did not significantly differ under any of these metrics (all $p > 0.1$), although there was a numerical trend for increased mean motion in patients (0.059 mm) compared to HCs (0.045 mm; $t_{(34)} = 1.60$, $p = 0.12$).

To ensure that the non-significant motion differences could not account for our results, we included 24 motion regressors to capture linear, quadatric, differential, and quadratic differential motion (S10, S11). Inclusion of these regressors did not qualitatively alter the

results. Both the critical group difference in the PreCue > PostCue contrast in the left posterior-VLPFC ($t_{(34)} = 2.32$, $p < 0.05$) and Lure > Control contrast in left mid-VLPFC ($t_{(34)} = 2.32$, $p < 0.05$) remained significant. Hence, it does not appear that motion confounded the present results.

Ruling Out General Working Memory Deficits

In a previous study, we found that patients with SZ could appropriately inhibit distractors prior to entry into working memory (WM), thereby ruling out an encoding or general maintenance deficit in WM (S12). However, as indicated in the main text, patients demonstrated increased error-rates relative to HCs even to Control probes in the present study. To examine whether the described patterns could be explained by a general WM deficit, we sub-sampled the patient group by excluding four participants demonstrating less than 90% accuracy on Control probes. Performance in the sub-sampled patient group (sSZ) was thus equated with that of HCs for Control probes (99.5% vs. 98.8%, $t_{(30)} = 0.8$, $p > 0.4$). Nevertheless, sSZs still demonstrated impaired performance on Lure probes relative to HCs ($t_{(30)} = 2.46$, $p < 0.05$) and the group difference in Lure compared to Control probes remained ($t_{(30)} = 2.34$, $p < 0.05$). Critically, group differences in the PreCue > PostCue contrast in posterior-VLPFC ($t_{(30)} = 2.09$, $p < 0.05$) and Lure > Control contrast in mid-VLPFC ($t_{(30)} = 3.45$, $p < 0.005$) remained. As a result, these patterns are unlikely to be due to a general WM deficit.

To further examine a potential general WM deficit, we examined activations in the posterior-VLPFC during Encoding and PreCue maintenance relative to a passive baseline. Deficient general WM processes would be expected to be reflected in reduced activation in patients relative to HCs. This pattern was not confirmed during either Encoding ($t_{(34)} = 0.09$, $p >$

0.9) or PreCue ($t_{(34)}$ = 0.82, p > 0.4). Hence, our data suggest that patient deficits are largely restricted to the PostCue phase and beyond, resulting from deficient inhibitory processes.

Encoding and PreCue Maintenance

The task was specifically designed to assess inhibition through the contrast of PreCue > PostCue and interference-control through the contrast of Lure > Control. However, previous research has documented deficient encoding and maintenance processes in patients with SZ (S13-S16). While our previous research with this and a related paradigm indicated intact encoding and maintenance (S12), it may nevertheless be instructive to investigate those phases in more detail. Due to the design, we did not have high level control conditions to contrast against Encoding and PreCue maintenance. As a result, we report here data from contrasts of these phases against a fixation baseline.

The contrast of Encoding > Baseline revealed widespread activation in visual cortices extending into the intra-parietal sulcus (IPS), as well as activations in medial and lateral frontal cortex (Figure S3A; Table S4). Direct comparison between groups revealed that HCs demonstrated increased activation in the right IPS relative to SZs. No areas demonstrated the reverse pattern. Targeted examination of each cluster activated across groups revealed no other group differences (all p > 0.1).

The contrast of PreCue > Baseline revealed activations in bilateral prefrontal and posterior parietal areas, as well as portions of occipital and temporal cortex (Figure S3B; Table S5). Direct comparisons between groups revealed no differences at a whole-brain corrected threshold. Targeted examination of each cluster activated across groups revealed increased

activation in the right IPS for HCs relative to SZs ($t_{(34)} = 2.44$, $p < 0.05$). No other comparison was significant (all $p > 0.15$).

Supplemental Discussion

While we have focused analysis on the VLPFC due to our prior hypotheses, comprehensive analyses revealed other regions that differ between patients with SZ and HCs during different phases of the task. Most notable, during Encoding and the PreCue maintenance interval, HCs demonstrated increased recruitment of the right IPS compared to patients. Although the contrasts revealing these effects were unconstrained due to the use of a simple resting baseline as a control condition, it is tempting to speculate on the role of the right IPS in the present study. Previous research has demonstrated that the IPS is a central node in the dorsal attention network (S17), playing a role in top-down attention and WM (S18). Through interactions with visual cortices, it is thought that the IPS is involved in binding object features (S19, S20). Here, the IPS may be important in binding word and color information. Reduced activation of the right IPS in patients with SZ may reflect impaired encoding and maintenance of color-word bindings. This could, in turn, lead to impaired use of color cues to discard irrelevant information from WM. We have previously demonstrated that patients with SZ have no difficulties in using color cues to guide encoding in WM (S12). Hence, patient deficits may be restricted to cases where bound information must be maintained in the absence of external stimulation. Examining the relationship between the binding functions of the IPS and control processes would be an interesting avenue for future research.

In addition to the left mid-VLPFC, patients with SZ also demonstrated increased activation in the dorsal anterior cingulate cortex and left premotor cortex in response to Lure

probes compared to Control probes. These areas are robustly activated across a variety of tasks that produce response conflict (S21). It is likely that patients' uncertainty with how to respond to Lure probes elicited response conflict. The activation of these areas may therefore be a reflection of this conflict.

Table S1. Whole-Brain Results: PreCue-PostCue

	region	area	x	y	z	voxels	peak z
All Subjects	left IFG - oper	44	-52	10	6	317	4.38
	left IFG - oper	44	-54	8	16		4.16
	left IFG - oper	44	-50	8	22		3.96
	left IFG - oper	44	-52	16	22		3.8
	left IFG - oper	44	-50	12	28		3.72
	left fusiform	37	-50	-66	-18	1647	6.36
	left IPS	7	-28	-62	44	5833	5.73
	right cerebellum		24	-64	-22	1708	5.64
	left STG	22	-62	-42	8	523	5.48
	left preMotor	6	-48	2	58	2239	5.43
	left preSMA	6	-2	4	62	192	4.87
	right ant DLPFC	46	40	50	24	133	4.19
HC Only	left IFG - oper	44	-48	8	20	1055	4.91
	left fusiform	37	-50	-66	-18	1577	5.79
	right fusiform	37	52	-62	-16	1529	5.57
	left MTG	21	-52	-48	12	428	5.43
	right IPS	7	32	-70	48	935	5.23
	left IPS	7	-24	-72	54	1230	4.82
	right PHG	30	14	-44	-2	414	4.57
	left lingual gyrus	18	-16	-92	-2	233	4.46
	left cuneus	19	-2	-92	36	1129	4.35
	left preCuneus	7	-4	-56	48	129	3.91
	right IFJ	6,44	48	8	34	99	3.86
SZ Only	left preMotor	6	-48	2	58	794	5.43
	left IPS	7	-28	-62	44	533	4.90
	left fusiform	37	-50	-68	-18	291	4.54
	right cerebellum		24	-60	-22	138	4.44
	right SOG	19	30	-78	38	81	4.09
HC > SZ	none						
SZ > HC	left temporal pole	38	-42	8	-22	183	4.50
	left ACC	32	-18	46	12	165	4.15

Coordinates of peak activation are reported in MNI space. Multiple sub-peaks are reported for the posterior ventrolateral prefrontal cortex since it was a site of *a priori* interest.

ACC, anterior cingulate cortex; ant, anterior; HC, healthy contols; IFG, inferior frontal gyrus; IFJ, inferior frontal junction; IPS, intraparietal sulcus; MFG, middle frontal gyrus; MNI, Montreal Neurological Institute; oper, pars opercularis; SMA, supplementary motor area; SOG, superior occipital gyrus; STG, superior temporal gyrus; SZ, patients with schizophrenia.

Table S2. Whole-Brain Results: Lure-Control

	region	area	x	y	z	voxels	peak z
All Subjects	left IFG - tria	45	-48	24	22	228	3.96
	left IFG - tria	45	-40	32	22		3.41
	left IFG - tria	45	-38	16	22		3.33
	left calcarine	17	-18	-68	8	517	4.89
	right dACC/preSMA	32,6	6	24	44	358	4.69
	left IPS	40	-40	-42	40	447	4.69
	left preMotor	6	-32	-4	36	402	4.65
	right preCuneus	7	8	-66	44	98	4.17
	right thalamus		12	-6	8	74	3.96
HC Only	left thalamus		-6	-20	8	435	4.82
	left preCuneus	7	-2	-62	40	343	4.67
	right calcarine	17	14	-68	6	146	4.28
SZ Only	left IFG - tria	45	-48	20	20	198	4.28
	left IPS	40	-42	-44	38	83	4.60
	left preMotor	6	-32	-4	36	217	4.57
	left dACC/preSMA	32,6	-8	16	50	275	4.57
	left IFG - orb	47	-46	18	-4	83	4.11
	left lingual gyrus	18	-22	-68	-8	75	3.78
HC > SZ	left thalamus		-4	-12	14	139	3.82
SZ > HC	none						

Coordinates of peak activation are reported in MNI space. Multiple sub-peaks are reported for the mid-ventrolateral prefrontal cortex since it was a site of *a priori* interest.

dACC, dorsal anterior cingulate cortex; HC, healthy controls; IFG, inferior frontal gyrus; IPS, intraparietal sulcus; MNI, Montreal Neurological Institute; orb, pars orbitalis; SMA, supplementary motor area; SZ, patients with schizophrenia; tria, pars triangularis.

Table S3. Within- and Between-Group Comparisons Outside Regions-of-Interest

PreCue-PostCue

region	peak	HC	SZ	HC vs SZ
left fusiform	-50 -66 -18	6.31***	4.45***	1.52
left IPS	-28 -62 44	7.77***	6.18***	0.93
right cerebellum	24 -64 -22	5.69***	3.71**	0.94
left STG	-62 -42 8	9.72***	3.93**	1.27
left preMotor	-48 2 58	8.10***	5.35***	-0.29
left preSMA	-2 4 62	4.28**	3.80**	-0.38
right ant DLPFC	40 50 24	3.98**	3.56**	0.01

Lure-Control

region	peak	HC	SZ	HC vs SZ
left calcarine	-18 -68 8	6.54***	4.66***	-0.29
right dACC/preSMA	6 24 44	3.71**	5.33***	-2.04*
left IPS	-40 -42 40	4.85***	4.47***	-1.24
left preMotor	-32 -4 36	3.27**	6.43***	-2.27*
right preCuneus	8 -66 44	5.32***	2.57*	1.38
right thalamus	12 -6 8	5.29***	2.55*	1.26

dACC, dorsal anterior cingulate cortex; DLPFC, dorsolateral prefrontal cortex; HC, healthy controls; IPS, intraparietal sulcus; SMA, supplementary motor area; STG, superior temporal gyrus; SZ, patients with schizophrenia.

*$p < 0.05$.

**$p < 0.005$.

***$p < 0.0005$.

Table S4. Encoding

Encoding-Baseline

	region	area	x	y	z	voxels	peak z	HC	SZ	HC vs SZ
All Subjects	parietal, occipital, temporal	18, 19, 7, 17, 37, 30, 40, 20, 21, 23, 36	-6	-88	-2	33597	7.82	12.65***	12.76***	1.48
	left preMotor, lat PFC	6, 9, 44, 45, 8	-46	2	32	3511	6.92	10.96***	7.49***	-1.2
	preSMA/dACC	6, 32	-2	6	60	979	6.79	7.23***	5.62***	-0.27
	right preMotor	6, 9	60	8	42	938	5.21	7.04***	5.25***	0.99
	right preMotor	6	68	-2	16	76	4.92	3.26**	3.57**	-0.5
	right ant DLPFC	10, 46	36	52	30	258	4.54	5.24***	2.68*	0.52
	right STS	22	-54	-36	4	116	4.23	3.19*	4.65***	-1.07
HC > SZ	right IPS	7, 40	38	-52	48	189	4.27			
SZ > HC	None									

dACC, dorsal anterior cingulate cortex; DLPFC, dorsolateral prefrontal cortex; HC, healthy controls; IPS, intraparietal sulcus; lat, lateral; PFC, prefrontal cortex; SMA, supplementary motor area; STS, superior temporal sulcus; SZ, patients with schizophrenia.

*$p < 0.05$.

**$p < 0.005$.

***$p < 0.0005$.

Table S5. PreCue

PreCue-Baseline

	region	area	x	y	z	voxels	peak z	HC	SZ	HC vs SZ
All Subjects	various	6, 7, 40, 9, 32, 18, 17, 22, 8, 44	-36	-42	40	25909	7.34	10.50***	12.34***	0.55
	left ant DLPFC	10, 46	-38	54	20	909	5.46	6.89***	5.18***	-1.47
	right ant DLPFC	10, 46	46	50	22	728	5.15	5.93***	4.19**	-1.23
	right IPS	40	40	-40	46	490	4.84	5.64***	2.31*	2.44*
	brainstem		-16	-18	-40	135	4.34	5.07***	3.75**	0.83
HC > SZ	None									
SZ > HC	None									

ant, anterior; DLPFC, dorsolateral prefrontal cortex; HC, healthy controls; IPS, intraparietal sulcus; SZ, patients with schizophrenia.
*$p < 0.05$.
**$p < 0.005$.
***$p < 0.0005$.

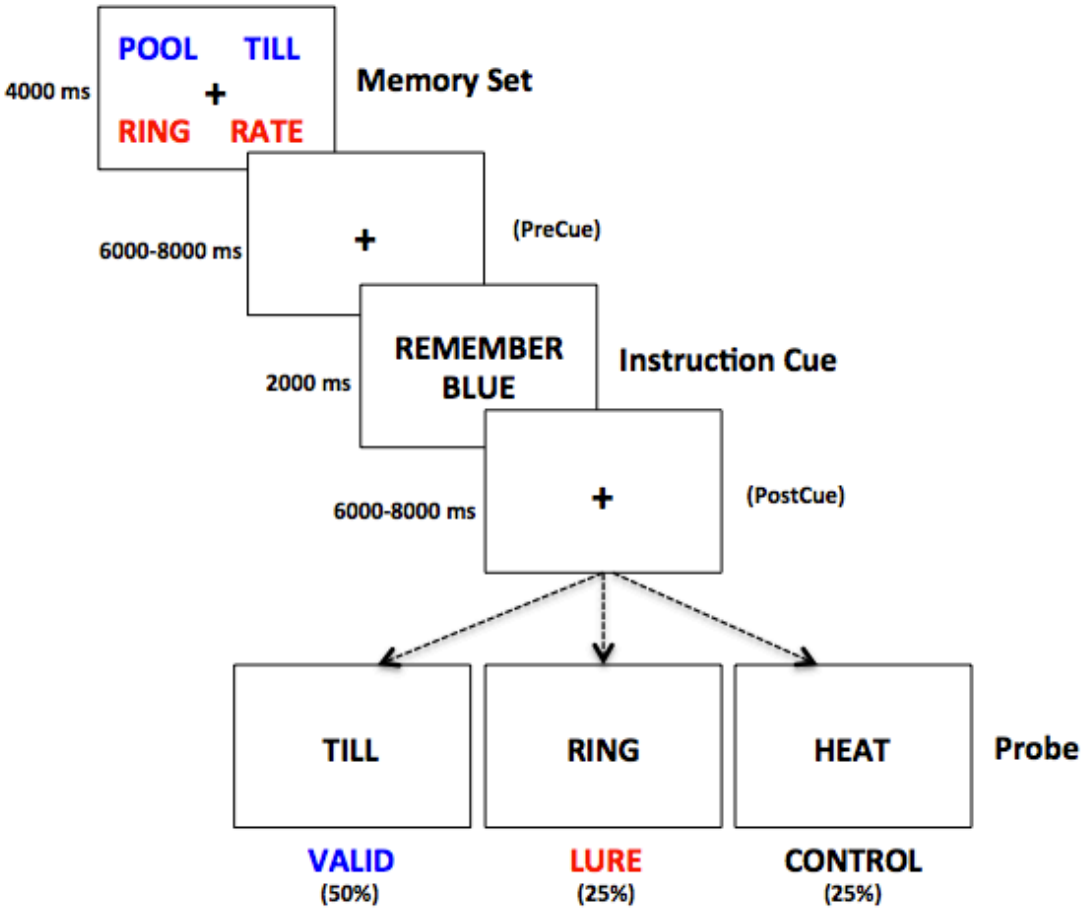

Figure S1. Task Schematic

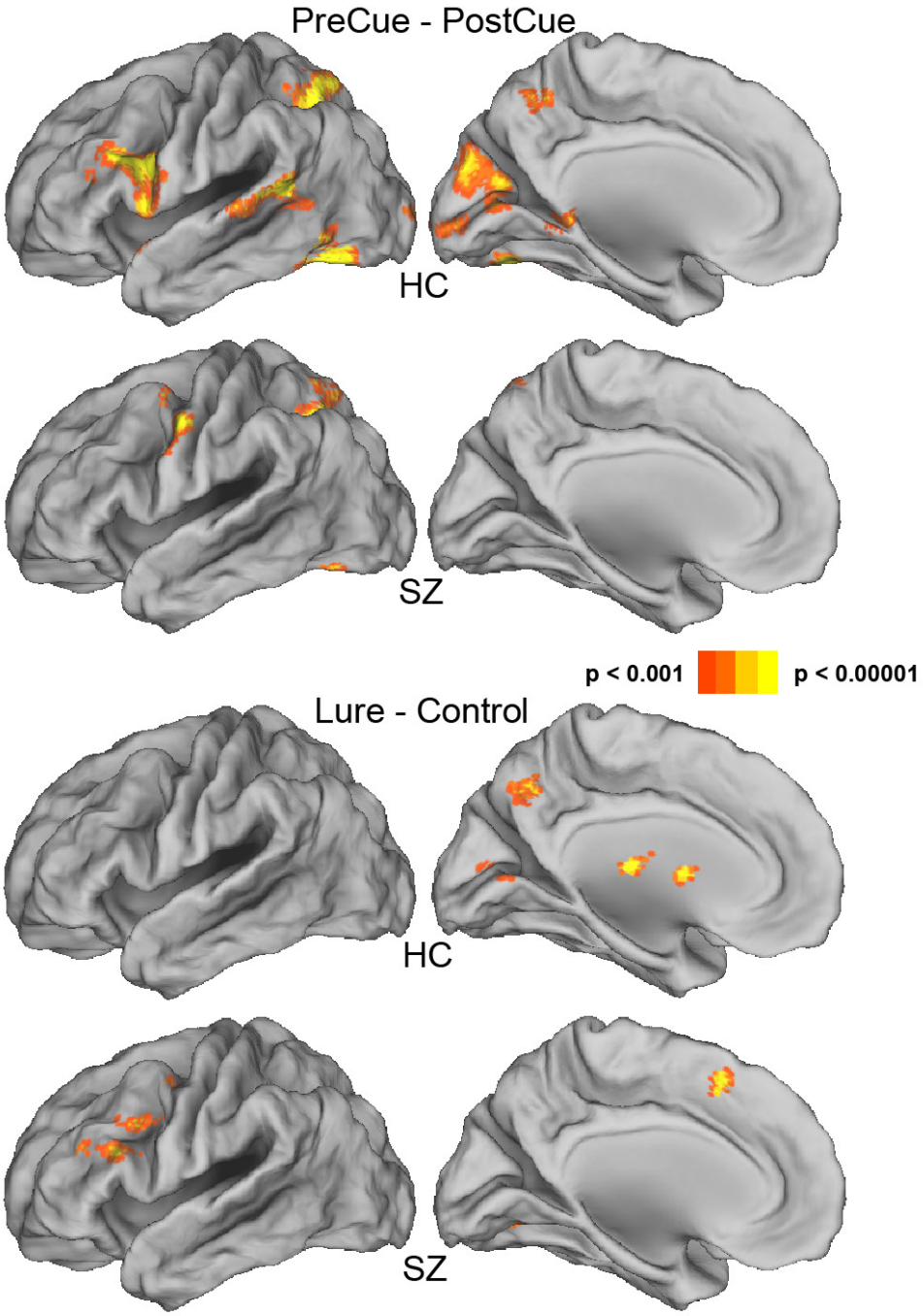

Figure S2. Top: Maintenance and inhibition-related activations (contrast of PreCue – PostCue activations) for healthy controls (HC) and patients with schizophrenia (SZ). Bottom: Interference-control related activations (contrast of Lure – Control probe activations) for HCs and patients with SZ.

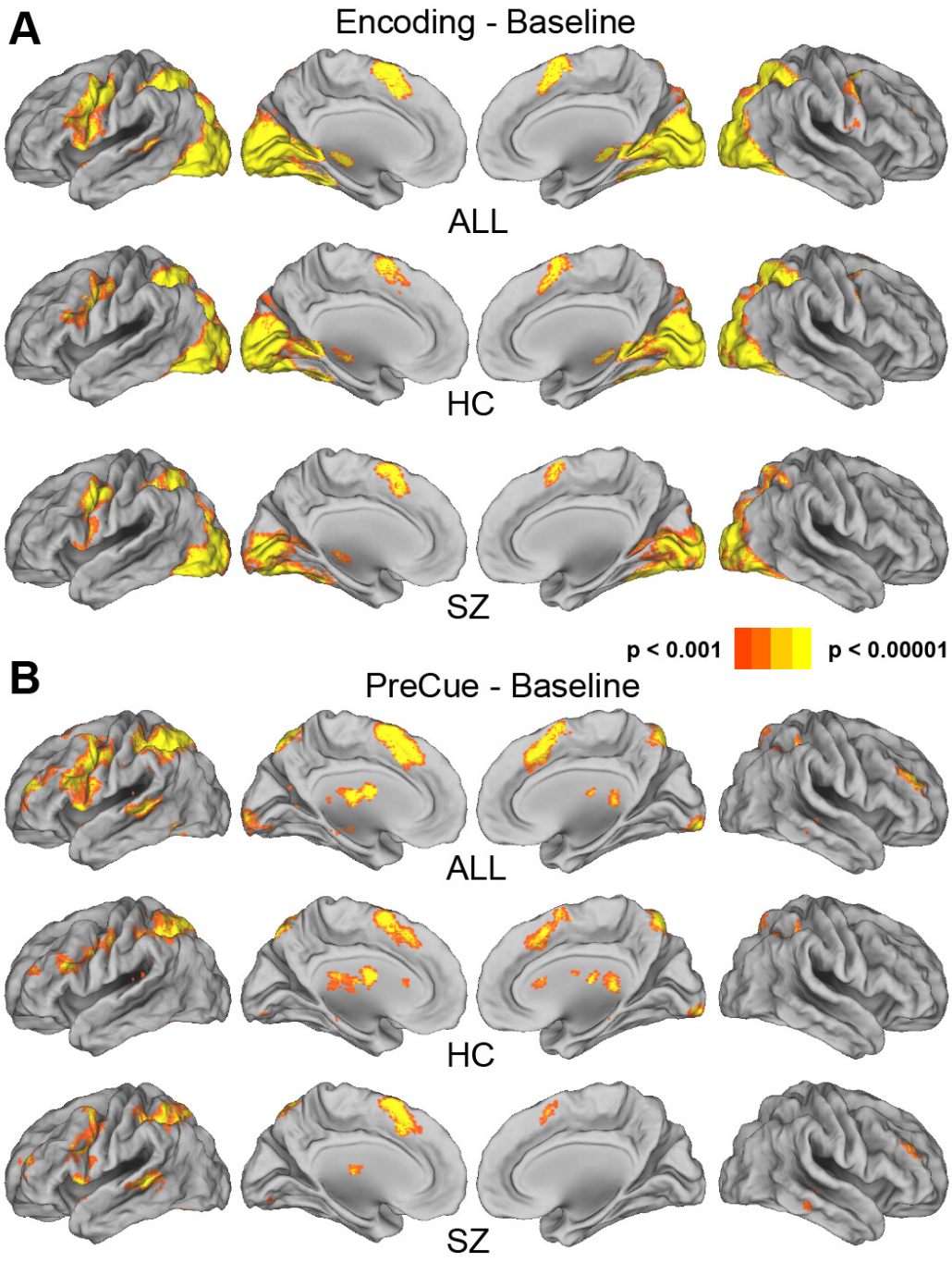

Figure S3. (**A**) Contrast of Encoding > Baseline for healthy controls (HC) and patients with schizophrenia (SZ). (**B**) Contrast of PreCue > Baseline for HCs and patients with SZ.

Supplemental References

S1. First MB, Spitzer RL, Gibbon M, Williams JBW (2007): *Structured Clinical Interview for DSM-IV-TR Axis I Disorders-Patient Edition* (SCID-I/P). New York: Biometrics Research, New York State Psychiatric Institute.

S2. Nurnberger JI Jr, Blehar MC, Kaufmann CA, York-Cooler C, Simpson SG, Harkavy-Friedman J, *et al.* (1994): Diagnostic interview for genetic studies. Rationale, unique features, and training. NIMH Genetics Initiative. *Arch Gen Psychiatry* 51:849-859; discussion 863-844.

S3. First MB, Pincus,HA (2002): The DSM-IV Text Revision: rationale and potential impact on clinical practice. *Psychiatr Serv* 53:288-292.

S4. Andreasen NC, & Olsen S (1982): Negative v positive schizophrenia. Definition and validation. *Arch Gen Psychiatry* 39:789-794.

S5. Addington D, Addington,J, Maticka-Tyndale E, Joyce J (1992): Reliability and validity of a depression rating scale for schizophrenics. *Schizophr Res* 6:201-208.

S6. Ashburner J, Friston K (1997): Multimodal image coregistration and partitioning-a unified framework. *Neuroimage* 6:209-217.

S7. Tzourio-Mazoyer N, Landeau B, Papathanassiou D, Crivello F, Etard O, Delcroix N, *et al.* (2002): Automated anatomical labeling of activations in SPM using a macroscopic anatomical parcellation of the MNI MRI single-subject brain. *Neuroimage* 1:273-89.

S8. Van Dijk KR, Sabuncu MR, Buckner RL (2012): The influence of head motion on intrinsic functional connectivity MRI. *Neuroimage* 59:431-8.

S9. Satterthwaite TD, Wolf DH, Loughead J, Ruparel K, Elliott MA, Hakonarson H, *et al.* (2012): Impact of in-scanner head motion on multiple measures of functional connectivity: relevance for studies of neurodevelopment in youth. *Neuroimage* 60:623-32.

S10. Satterthwaite TD, Elliott MA, Gerraty RT, Ruparel K, Loughead J, Calkins ME, *et al.* (2013): An improved framework for confound regression and filtering for control of motion artifact in the preprocessing of resting-state functional connectivity data. *Neuroimage* 64:240-56.

S11. Lund TE, Nørgaard MD, Rostrup E, Rowe JB, Paulson OB (2005): Motion or activity: their role in intra- and inter-subject variation in fMRI. *Neuroimage* 26:960-4.

S12. Smith EE, Eich TS, Cebenoyan D, Malapani C (2011): Intact and impaired cognitive-control processes in schizophrenia. *Schizophr Res* 126:132-137.

S13. Anticevic A, Repovs G, Barch DM (2011): Working memory encoding and maintenance deficits in schizophrenia: neural evidence for activation and deactivation abnormalities. *Schizophr Bull* 39:168-78.

S14. Anticevic A, Repovs G, Corlett PR, Barch DM (2011): Negative and non-emotional interference with visual working memory in schizophrenia. *Biol Psychiatry* 70:1159-68.

S15. Johnson MR, Morris NA, Astur RS, Calhoun VD, Mathalon DH, Kiehl KA, Pearlson GD (2006): A functional magnetic resonance imaging study of working memory abnormalities in schizophrenia. *Biol Psychiatry* 60:11-21.

S16. Driesen NR, Leung H-C, Calhoun VD, Constable RT, Gueorguieva R, Hoffman R, *et al.* (2008): Impairment during working memory maintenance and response in schizophrenia: functional magnetic resonance imaging evidence. *Biol Psychiatry* 64:1026-34.

S17. Corbetta M, Shulman GL (2002): Control of goal-directed and stimulus-driven attention in the brain. *Nat Rev Neurosci* 3:201-15.

18. Chun MM, Golomb JD, Turk-Browne NB (2011): A taxonomy of external and internal attention. *Annu Rev Psychol* 62:73–101.

S19. Shafritz KH, Gore JC, Marois R (2002): The role of the parietal cortex in visual feature binding. *Proc Natl Acad Sci U S A* 99:10917–10922.

S20. Ptak R (2012): The frontoparietal attention network of the human brain action, saliency, and a priority map of the environment. *Neuroscientist* 18:502-515.

S21. DE Nee, TD Wager, J Jonides (2007): Interference resolution: Insights from a meta-analysis of neuroimaging tasks. *Cogn Affect Behav Neurosci* 7:1-17.